Journal of
Nanoelectronics and Optoelectronics
Vol. 6, 473–477, 2011

Photoluminescence and Raman Study of Well-Aligned ZnO Nanorods on *p*-Si Substrate

V. V. Ursaki[1,*], O. Lupan[2,3], I. M. Tiginyanu[4], G. Chai[3], and L. Chow[3]

[1] Institute of Applied Physics, Academy of Sciences of Moldova, MD-2028 Chisinau, Republic of Moldova
[2] Department of Microelectronics and Semiconductor Devices, Technical University of Moldova, 168 Stefan cel Mare Blvd., Chisinau, MD-2004, Republic of Moldova
[3] Department of Physics, University of Central Florida, Orlando, PO Box 162385, FL, USA
[4] Institute of Electronic Engineering and Nanotechnologies, Academy of Sciences of Moldova, MD-2028 Chisinau, Republic of Moldova

We report on optical properties of ZnO nanorods grown on *p*-type Si substrates by an electric-field assisted assembly technique in aqueous solutions applied at relative low temperature (96 °C). The results of micro-Raman study are indicative of high crystalline quality of the produced nanorods. The analysis of the photoluminescence properties of the material demonstrates the possibility to control the free carrier concentration by post-growth thermal treatment leading to the formation of compensating centers, while the crystalline quality of the material is not affected.

Keywords: ZnO Nanorod Arrays, Self-Assembly, Electric Field Assisted Growth, Photoluminescence Properties.

1. INTRODUCTION

ZnO demonstrates increasing fundamental interest and widening of high-technology applications due to its wide and direct band gap (3.37 eV at 300 K), large exciton binding energy (60 meV), large bond strength (with a cohesive energy of 1.89 eV), and large mechanical stability (with a melting point of about 2200 K).[1] It is of a particular interest for photonic devices,[2] ultra-violet lasers,[3] nanosensors[4] and light emitting diodes[5,6] with higher performances and significantly lower cost. ZnO nanorods/nanowires are becoming common building blocks for the next generation of electronic devices[4] due to their superior properties compared to the bulk material, such as high crystalline quality, large aspect ratio, and quantum confinement effects.[7–9] Yang et al. have recently pointed out on the importance of the development of new fabrication techniques for the preparation of nanorods arrays and their integration in devices.[8] In this sense, chemical methods with electric field assisted assembly offer new opportunities for the production of heterostructures in nanodevices and multicomponent systems based on nanorod arrays with high performances and a significantly lower cost in comparison to the traditional lithographic techniques. The manipulation and positioning of zinc oxide nanorods is a key challenge toward the integration of nanostructures in larger scale systems.

ZnO nanoarchitectures can be assembled on different substrates (e.g., glass, silicon, sapphire) by patterning a seed or catalyst layer.[3] Usually, gold is used to catalyze the growth of nanorods with vapor–liquid–solid (VLS) methods, while silver is used to facilitate the assembly of ZnO nanorods from solutions.[10,11]

In this paper, we investigate the photoluminescence and Raman properties of electric field assisted growth of aligned ZnO nanorods on *p*-silicon substrate.

2. EXPERIMENTAL DETAILS

The hydrothermal synthesis of vertically-aligned ZnO nanorod arrays was carried out by dissolving zinc sulfate and ammonia in 20 mL of deionized water (18.2 MΩ · cm). Commercial $Zn(SO_4) \cdot 7H_2O$ (99.9% purity) and NH_4OH (29.6%) were used without additional purification. The complex solution was then transferred to a reactor.[12] A DC electric field was applied during the growth procedure. The substrates, Si or glass slides, were placed in vertical or horizontal positions in order to study the effect of the electric field direction on the morphology of the synthesized samples.[13] The reactor was held at 96 °C for 20 min and then cooled down to 40 °C.

*Author to whom correspondence should be addressed.

 1555-130X/2011/6/473/005 doi:10.1166/jno.2011.1198

After synthesis, the substrates were washed with distilled water several times and then dried in a hot air flux at 150 °C. In order to investigate the effect of the thermal treatment on the properties of the produced material, the samples were subjected to annealing at different temperatures for 1 h in air. The morphology and the chemical composition of zinc oxide samples were studied using a VEGA TESCAN TS 5130MM scanning electron microscope (SEM) equipped with an Oxford Instruments INCA energy dispersive X-ray (EDX) system. The EDX analysis of the material indicated a stoichiometric ZnO composition (within a precision of 1 at%).

The continuous wave (cw) photoluminescence (PL) was excited by the 351.1 nm line of an Ar^+ Spectra Physics laser and analyzed with a double spectrometer ensuring a spectral resolution better than 0.5 meV. The samples were mounted on the cold station of a LTS-22-C-330 optical cryogenic system. The room temperature Raman scattering was investigated with a MonoVista CRS Confocal Laser Raman System in the backscattering geometry under the excitation by a 532 nm DPSS laser.

3. RESULTS AND DISCUSSION

SEM image in Figure 1 illustrates ZnO nanorods grown on a *p*-Si(111) substrate under the assistance of a relatively weak electric field ($\sim 7 \cdot 10^3$ V/m) directed perpendicularly to the substrate surface. One can observe that the nanorods are predominantly oriented perpendicularly to the substrate surface. The alignment of ZnO nanorods improves with increasing the electric field strength ($\sim 6 \cdot 10^4$ V/m), as shown in the insert of Figure 1. One should note that the nanorods grown without any electric fields, or with the electric field oriented parallel to the substrate surface, are highly disordered (not shown here). The analysis of the image presented in Figure 1 reveals a hexagonal symmetry of the produced ZnO nanorods and a mean diameter of the nanorods around 250 nm.

The perpendicular orientation of the ZnO nanorods is controlled by the electric field, but the lattice match with the substrate may play a role in the growth process. The lattice mismatch between ZnO and Si(111) is ~3.5%.[14] By comparing the growth on various substrates, we observed a better uniformity and vertical alignment of ZnO nanorods grown on Si as compared to quartz substrates.

In order to study the vibrational properties of the ZnO nanorod arrays room-temperature Raman measurements were performed. Figure 2 shows the micro-Raman spectrum of ZnO nanorods grown on Si substrates with an applied electric field of $6 \cdot 10^4$ V/m. The wurtzite phase ZnO belongs to C_{6v}^4 or $P6_3mc$ symmetry group. The observed peaks are assigned to phonon modes of the wurtzite-type ZnO, except for the peaks at 521 cm^{-1} and 303 cm^{-1} which come from the Si substrate.[15, 16] According to the group theory, the corresponding zone center optical phonons are $\Gamma_{opt} = 1A_1 + 2B_1 + 1E_1 + 2E_2$.[17] The $A_1 + E_1 + 2E_2$ modes are Raman active, while $2B_1$ are silent. A_1 and B_1 modes are polar and split into transverse optical (TO) and longitudinal optical (LO) phonons. The low-frequency E_2 mode is predominantly associated with the non-polar vibration of the heavier Zn sublattice, while the high frequency E_2 mode involves predominantly the lighter oxygen atoms. The peak at 332 cm^{-1} is attributed to the $E_{2H} - E_{2L}$ second order Raman processes. The strong E_2(low) and E_2(high) peaks at 100 cm^{-1} and 438 cm^{-1}, respectively, demonstrate that the produced ZnO nanorods are of good crystalline hexagonal structure. The high crystalline quality is also indicated by a very narrow linewidth of the E_2(low) peak. The position of the E_2(high)

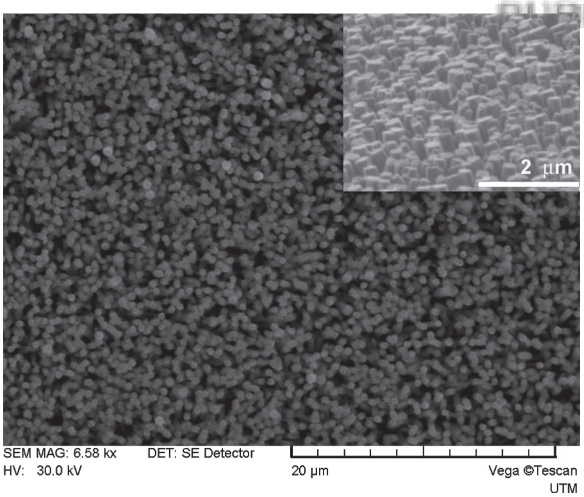

Fig. 1. SEM images of quasi-aligned ZnO nanorods on *p*-Si substrate grown under electric field assisted-assembly. Insert shows a 65°-tilted view of the ZnO nanorods on *p*-Si substrate grown under stronger electric field.

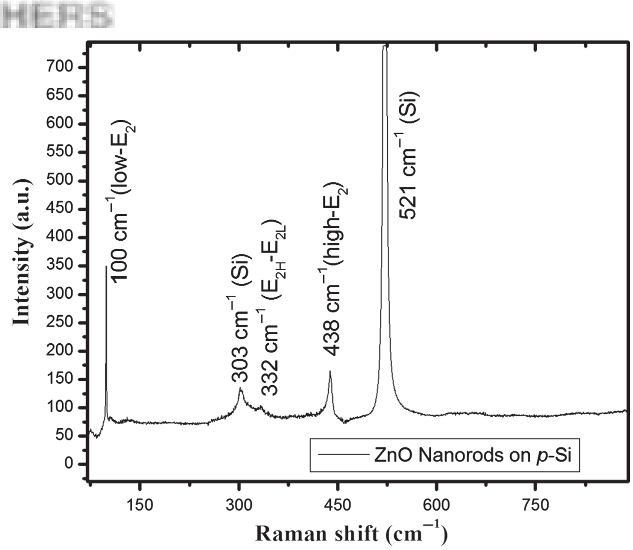

Fig. 2. Micro-Raman scattering spectrum of quasi-aligned ZnO nanorods on *p*-Si wafers grown under electric field assisted-assembly.

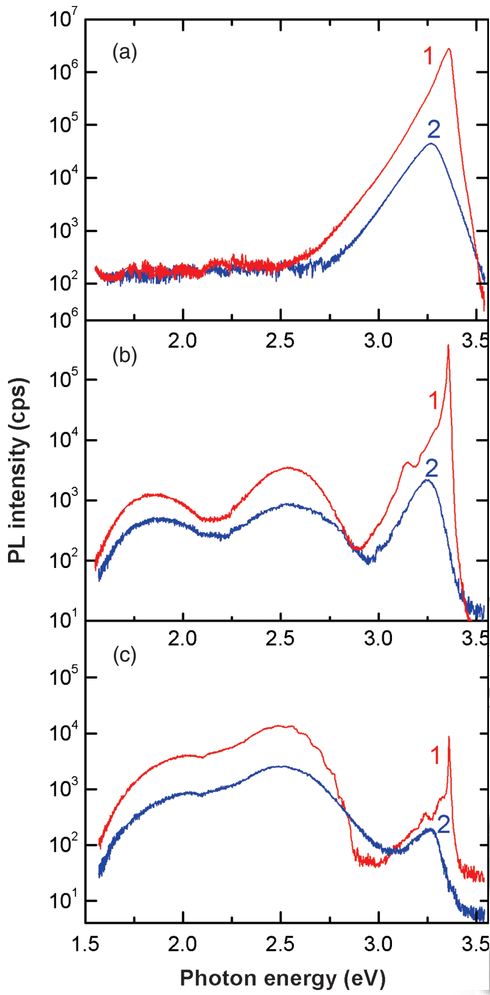

Fig. 3. PL spectrum of the: (a) as-grown sample, (b) the sample annealed at 400 °C during 1 h in air, and (c) the sample annealed at 800 °C during 1 hour in air. The spectra are measured at $T = 10$ K (curve 1), and $T = 300$ K (curve 2).

mode, situated close to that of bulk ZnO (437–439 cm^{-1}), is indicative of the unstrained state of ZnO nanorods.

The photoluminescence spectrum of the as-grown samples (Fig. 3(a)) consists of a very intensive near bandgap band with the maximum at 3.36 eV for $T = 10$ K, and 3.27 eV for room temperature. No visible emission is observed in the sample (at least at the level four orders of magnitude less that the intensity of the near bandgap luminescence). Thermal annealing at 400 °C for 1 h in air (Fig. 3(b)) leads to decreasing of the intensity of the near bandgap luminescence by almost an order of magnitude, a significant narrowing of this PL band, and the emergence of two visible PL bands at 2.55 eV and 1.85 eV. The increase of the annealing temperature to 800 °C (Fig. 3(c)) results in a further decrease of the intensity of the near bandgap luminescence by an additional order of magnitude with its further narrowing, and in further increase of the visible emission. We will discuss first the possible nature of the near bandgap PL band in the as prepared samples.

A characteristic feature of this near-band-gap PL band is the broadening towards the Stokes part of the emission. The width of this PL band is 57 meV at 10 K and 142 meV at room temperature. Several mechanisms that may contribute to the broadening of this PL band have been previously discussed.[18–21] It was shown that most probably this PL band is due to direct transitions of electrons between the conduction to valence band tails. The broadening of the PL band involved can be accounted for by the broadening of the band edges due to potential fluctuations induced by the high concentration of intrinsic defects or impurity. The width of the band tails, and the dependence of the full width at half maximum (FWHM) of the PL band on carrier concentration, can be calculated using the model for broadening of impurity bands in heavily doped semiconductors developed by Morgan.[22] This model has been applied to correlate the width of the PL band to the free carrier concentration in highly doped ZnO samples.[18–20] By using the established dependence, one can estimate that the electron concentration in our as prepared samples is 3.9×10^{19} cm^{-3} at $T = 10$ K, and 2.2×10^{20} cm^{-3} at room temperature.

As concerns the microscopic origin of the impurity responsible for the potential fluctuations which cause broadening of the PL band, most probably it is related to residual impurities of the III group of the periodic table, or to the hydrogen, which are known to be shallow donors in ZnO.[23,24] As concerns the contribution from native defects, it seems to be insignificant. Oxygen vacancies and zinc interstitials are the most probable donor-type intrinsic defects.[25,26] Oxygen vacancy is a deep donor, while zinc interstitials are not stable at room temperature and so are unlikely to contribute to the carrier concentration.[27]

In order to analyze in more details the evolution of the near bandgap luminescence, Figure 4 presents the temperature dependence of the near bandgap PL spectra in as prepared and annealed samples.

Annealing of samples at 400 °C leads to a change on the nature of the near bandgap luminescence, it being dominated by the recombination of donor bound excitons (D^0X) with LO phonon replica. The width of the PL band cannot be anymore used for the estimation of the free carrier concentration. The zero-phonon D^0X line is situated at 3.356 eV. A weaker PL band due to the recombination of donor acceptor pairs is also observed in the spectra.

Annealing at 800 °C leads to a further decrease of the free carrier concentration, the decrease of the intensity of the D^0X luminescence and the emergence of luminescence related to the recombination of free excitons (FX), as illustrated in Figure 4(c). The $(D^0X)_{2e}$ line at 3.319 eV is a two-electron replica of the D^0X line. The two-electron-satellite separation of this neutral donor bound exciton in our crystals is 37 meV, which implies that the related donor binding energy is equal to 49 meV.

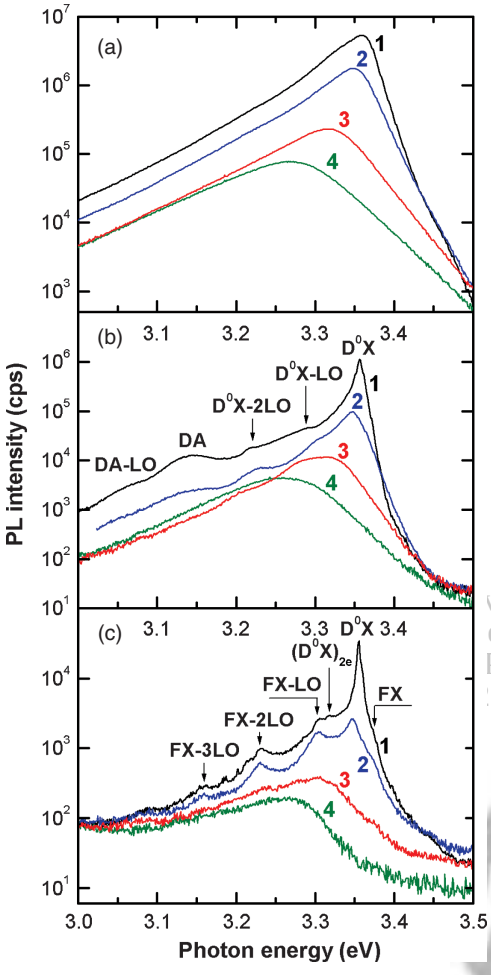

Fig. 4. Near bandgap PL spectrum of the: (a) as-grown sample; (b) the sample annealed at 400 °C during 1 h in air, and (c) the sample annealed at 800 °C, 1 h in air. The spectra are measured at $T = 10$ K (curve 1), $T = 100$ K (curve 2), $T = 200$ K (curve 3), and $T = 300$ K (curve 4).

Therefore, the decrease of the near bandgap luminescence intensity and the increase of the visible luminescence intensity caused by annealing, accompanied by an essential narrowing of the near bandgap PL bands, are indicative of the creation of deep acceptor centers which compensate the free electron concentration. On the other hand, the narrowing of the PL lines suggests that annealing does not affect the crystalline quality of the material. The analysis of the visible emission suggests that deep acceptor centers are created predominantly by the annealing. The PL band at 1.85 eV was previously suggested to be related to the recombination of free electrons with holes localized at a deep acceptor with the energy level situated in the middle of the bandgap, while the band at 2.5–2.6 eV was assigned to either zinc vacancy or Cu impurity acceptors.[28] The fine structure of the green PL band revealed in samples annealed at 800 °C may be attributed to the annealing induced activation of the residual Cu impurity, since the structured green PL band with the zero-phonon transition around 2.85 eV is usually attributed to the Cu impurity.[28]

4. CONCLUSIONS

The results of this study demonstrate the possibilities to control through thermal treatment the physical properties of vertically-aligned ZnO nanowires produced by an electric-field assisted assembly technique in aqueous solutions. Well aligned ZnO nanowires were synthesized without employing any seed layer or metal catalysts on Si(111) substrates. According to the analysis of photoluminescence spectra, the electron concentration in the as prepared samples is 3.9×10^{19} cm^{-3} at $T = 10$ K, and 2.2×10^{20} cm^{-3} at room temperature. The post-growth thermal treatment leads to an essential decrease of the free carrier concentration indicated by a sharp narrowing the near-bandgap PL lines, which is also indicative of the preservation, or even improvement, of the crystalline quality. The decrease of the electron concentration induced by annealing is explained by the creation of deep acceptor compensating centers deduced from the increase of the intensity of visible PL bands with maxima at 1.85 and 2.55 eV. The emergence of a fine structure of the green PL band in samples annealed at high temperatures (800 °C) is considered to be an indicative of the activation of the residual Cu impurity, which contributes to the compensation of the free electron concentration.

Acknowledgment: Dr. V. V. Ursaki acknowledges financial support by the Academy of Sciences of Moldova under the State Programme "Nanotechnologies and nanomaterials," Grant No. 09.836.05.07F.

References and Notes

1. S. Tuzemen and E. Gur, *Opt. Mater.* 30, 292 (**2007**).
2. S. Choopun, H. Tabata, and K. Kawai, *J. Cryst. Growth* 274, 167 (**2005**).
3. M. Huang, S. Mao, H. Feick, H. Yan, Y. Wu, H. Kind, E. Weber, R. Russo, and P. Yang, *Science* 292, 1897 (**2001**).
4. O. Lupan, G. Chai, and L. Chow, *Microelectronic J.* 38, 1211 (**2007**).
5. X. F. Duan, Y. Huang, Y. Cui, J. F. Wang, and C. M. Lieber, *Nature* 409, 66 (**2001**).
6. R. Hauschild and H. Kalt, *Appl. Phys. Lett.* 89, 123107 (**2006**).
7. Z. L. Wang, *Mater. Sci. Eng. R* 64, 33 (**2009**).
8. P. Yang, R. Yan, and M. Fardy, *Nano Lett.* 10, 1529 (**2010**).
9. M. Yan, H . T. Zhang, E. J. Widjaja, and R. P. H. Chang, *J. Appl. Phys.* 94, 5240 (**2003**).
10. J. Henzie, J. Barton, C. Stender, and T. Odon, *Acc. Chem. Res.* 39, 249 (**2006**).
11. J. W. P. Hsu, Z. R. Tian, N. C. Simmons, C. M. Matzke, J. A. Voigt, and J. Liu, *Nano Lett.* 5, 83 (**2005**).
12. O. Lupan, L. Chow, G. Chai, B. Roldan, A. Naitabdi, A. Schulte, and H. Heinrich, *Mater. Sci. Eng.: B* 145, 57 (**2007**).
13. O. Lupan, L. Chow, G. Chai, S. Park, and A. Schulte, *Technical Proceedings of the 2008 NSTI Nanotechnology Conference and Trade Show, NSTI-Nanotech, Nanotechnology* (**2008**), Vol. 1, p. 567.
14. A. Nahhas, H. K. Kim, and J. Blachere, *Appl. Phys. Lett.* 78, 1511 (**2001**).
15. K. A. Alim, V. A. Fonoberov, M. Shamsa, and A. A. Balandin, *J. Appl. Phys.* 97, 124313 (**2005**).

16. M. Rajalakshmi, A. K. Arora, B. S. Bendre, and S. Mahamuni, *J. Appl. Phys.* 87, 2445 **(2000)**.
17. C. Bundesmann, N. Ashkenov, M. Schubert, D. Spemann, T. Butz, E. M. Kaidashev, M. Lorenz, and M. Grundmann, *Appl. Phys. Lett.* 83, 1974 **(2003)**.
18. V. V. Ursaki, I. M. Tiginyanu, V. V. Zalamai, E. V. Rusu, G. A. Emelchenko, V. M. Masalov, and E. N. Samarov, *Phys. Rev. B* 70, 155204 **(2004)**.
19. V. V. Zalamai, V. V. Ursaki, E. V. Rusu, P. Arabadji, I. M. Tiginyanu, and L. Sirbu, *Appl. Phys. Lett.* 84, 5168 **(2004)**.
20. V. V. Ursaki, O. I. Lupan, L. Chow, I. M. Tiginyanu, and V. V. Zalamai, *Solid St. Commun.* 143, 437 **(2007)**.
21. E. Iliopoulos, D. Doppalopudi, H. M. Ng, and T. D. Moustakas, *Appl. Phys. Lett.* 73, 375 **(1998)**.
22. T. N. Morgan, *Phys. Rev.* 139, A343 **(1965)**.
23. B. K. Meyer, H. Alves, D. M. Hofmann, W. Kriegseis, D. Forster, F. Bertram, J. Christen, A. Hoffmann, M. Straßburg, M. Dworzak, U. Haboeck, and A. V. Rodina, *Phys. Stat. Sol. (b)* 241, 231 **(2004)**.
24. Y. B. Zhang, G. K. L. Goh, K. F. Ooi, and S. Tripathy, *J. Appl. Phys.* 108, 083716 **(2010)**.
25. B. Zhang, S. H. Wei, and A. Zunger, *Phys. Rev. B* 63, 075205 **(2001)**.
26. E. Oba, S. R. Nishitani, S. Isotani, H. Adachi, and I. Tanaka, *J. Appl. Phys.* 90, 824 **(2001)**.
27. M. D. McCluskey and S. J. Jokela, *J. Appl. Phys.* 106, 071101 **(2009)**.
28. Ü. Özgür, Y. I. Alivov, C. Liu, A. Teke, M. A. Reshchikov, S. Doğan, V. Avrutin, S.-J. Cho, and H. Morkoç, *J. Appl. Phys.* 98, 041301 **(2005)**.

Received: 31 March 2011. Accepted: 28 April 2011.